Palestine Journal of Mathematics

Vol. 12(Special Issue IV)(2023) , 33–44

A numerical approach for solving Thomas–Fermi type equations using nonpolynomial B-spline function

Geetan Manchanda, Zainav Khatoon and Mohammad Prawesh Alam*

2000 Mathematics Subject Classification: 65L10 65L60 34B16..

Keywords and phrases: Non-linear boundary value problems, Uniform Algebraic Trigonometric tension B-spline functions, Error analysis.

The authors are thankful to the Prof. Arshad Khan for reading manuscript and suggesting his valuable comments, which improved the quality of the manuscript.

Abstract In this work, we have devised a high order numerically trustworthy computational technique for solving the generalised Thomas-Fermi boundary value problems. The method is based on uniform algebraic trigonometric tension B-spline basis functions and employs uniform algebraic trigonometric tension. This method annihilates singular behaviour at the point $d = 0$ and handles problems very easily. We have accomplished two numerical problems in order to demonstrate the effectiveness and robustness of the method, as well as to validate the results obtained from the theoretical analysis. It is shown that the new method works better than the old ones because it is easy to use and is computationally cost effective.

1 Introduction

An study into the effective nuclear charge in heavy atoms gave way to a well-known non-linear differential equation called the Thomas-Fermi equation [1, 2]. This equation is known as the Thomas-Fermi equation. Thomas and Fermi conducted the first tests on it in what is known as a semi-infinite interval, which is explained further below:

$$\begin{cases} W''(d) - d^{-1/2}Y^{3/2}(d) = 0, \quad d \in [0, \infty) \\ \lim_{d\to\infty} W(d) = 0, W(0) = 1. \end{cases} \tag{1.1}$$

It is helpful for computing form factors and achieving good potentials that can be applied as initial test potentials in self-consistent field calculations. It can also be used to investigate electrons in metals and nucleons in atomic structures. However, boundary conditions play a vital role in calculating the various properties of the atom. As a result, for convenience, the vast majority of research is carried out for finite intervals rather than a semi-infinite span. The fundamental objective of this study is to create a numerical approach employing uniform algebraic trigonometric (UAT) tension B-spline basis functions for a large class of Thomas–Fermi type equations with boundary conditions of the kind that is described in the following sentence:

$$\begin{cases} (q(d)W'(d))' = p(d)g(d, W(d)), \quad d \in (0, 1) \\ W'(0) = \alpha, \omega_1 W(1) + \omega_2 W'(1) = \omega_3. \end{cases} \tag{1.2}$$

with $\omega_1 > 0, \omega_2, \omega_3$ are finite constants. Here $q(d) = d^n W(d)$, $W(d) \neq 0$, $p(d) = d^m t(d)$, $t(d) \neq 0$, $q(0) = 0$ and $p(d)$ is not continuous at $d = 0$. In order to demonstrate that the existence and uniqueness of the solution to the problem (1.2) we make the following assumptions on and $g(d, W(d))$:

(i) The function $g(z, W(z), q(z)W'(z))$ is continuous,

(ii) $\frac{\partial g}{\partial W}$ and $\frac{\partial g}{\partial W'}$ exist and continuous,

(iii) $\frac{\partial g}{\partial W} \geq 0$ and $|\frac{\partial g}{\partial W'}| \leq K$, for some positive constant K.

Aforementioned constraints make sure that the problem exists and is unique (1.2), but there are other boundary conditions that have been discussed about in [3, 4, 5, 6, 7]. Strongly nonlinear boundary value problems (BVPs) are hard to solve exactly because they have a singularity at $d = 0$ and a significant amount of nonlinearity embedded inside the source function $g(d, W(d))$. So, it's important to come up with a high-order, reliable, and effective numerical method for solving the problem (1.2). In the literature review, we have gotten rid of a number of authors' numerical methods for solving Thomas-Fermi nonlinear singular BVPs that are easy on the computer and work well. In [8, 9, 10], the authors developed numerical technique by using finite difference method(FDM). Various authors developed numerical technique by using spline basis function [11, 12, 13, 14, 15, 16, 17, 18, 19, 20], Mickens' type non-standard FDM [21] and non-standard FDM [22]. Moreover, a number of researcher have come up with a variety of other computational strategies, such as the variational iteration method [23], the interpolation approach using hermite functions [24], the inverse integral operator with adomian decompostion method (ADM) [25], the interpolation scheme using the sinc function [26] etc. Moreover, authors in [27, 28, 29], have devised concise approaches based on finite differences for the solution of the problem (1.2) with $q(d) = p(d) = d^{\alpha}r(d)$ and $g(d, W(d), q(d)W(d))$= $g(d, W(d))$. In contrast, many authors have written about numerical methods that use polynomial basis functions and wavelet methods, including the interpolation method that employs the Laguerre wavelet [30], the improved decomposition technique that employs Green's functions [31], the numerical method that is focused on traditional algebraic expressions [32], the interpolation technique that employs the Haar-wavelet [33], and the integrated intelligent computing method that makes use of neural networks [34]. It is important to note that very few computational approaches for solving non-linear SVBP have been established in the literature. For instance, the authors of the study [13] created two numerical approaches for tackling problems based on uniform and nonuniform meshes that made use of cubic B-splines (1.2). For the purpose of resolving SBVPs, the authors of paper [35, 36, 37, 38], created a numerical technique that is based on an accretion of ADM and an approach using Green's function. Inspired and motivated by the preceding research, we want to determine a numerical approximation of the Thomas-Fermi equation. In order to grasp highgrade precision, overcome the singularity, and establish the stability of an approximate solution to a class of Thomas-Fermi equation, we have provided a numerical approach that is based on the UAT tension B-spline interpolation scheme. The remaining article is arranged in the following form: In section 2, we discuss the collocation method using the UAT tension B-spline collocation method for solving (1.2). In section 3, we used some numerical examples to demonstrate the relevance of the proposed method. In section 4, we will wrap up our work.

2 Construction of the suggested algorithm

In this article, we design a numerical approach employing the UAT tension B-spline interpolation algorithm in order to approximate the solution of the problem that has been examined (1.2). In order to do this, we will first rewrite the equation (1.2) as follows:

$$W''(d) + \left(\frac{\eta}{d} + \frac{q'(d)}{q(d)}\right)W'(d) = \frac{p(d)}{q(d)}g(d, W(d)), \quad d \in [0, 1]. \tag{2.1}$$

Since the equation (2.1) contains a singularity at the point $d = 0$, we have applied the L'Hospital rule to the first derivative term in order to get around the singularity. Hence, at $d = 0$ equation (2.1) becomes:

$$(1+\eta)W''(d) + \frac{q'(d)}{q(d)}W'(d) = \frac{p(d)}{q(d)}g(d, W(d)), \tag{2.2}$$

and at $0 < d \leq 1$, equation (2.1), becomes:

$$W''(d) + \left(\frac{\eta}{d} + \frac{q'(d)}{q(d)}\right)W'(d) = \frac{p(d)}{q(d)}g(d, W(d)). \tag{2.3}$$

Combining equations (2.2) and (2.3), we have

$$Q(d)W''(d) + P(d)W'(d) = \frac{p(d)}{q(d)}g(d, W(d)) \tag{2.4}$$

with boundary conditions

$$W'(0) = 0, \text{ and } \omega_1 W(1) + \omega_2 W'(1) = \omega_3, \tag{2.5}$$

where

$$Q(d) = \begin{cases} 1+\eta, & d = 0 \\ 1, & \text{otherwise.} \end{cases} \tag{2.6}$$

and

$$P(d) = \begin{cases} \frac{q'(d)}{q(d)}, & d = 0 \\ \frac{\eta}{d} + \frac{q'(d)}{q(d)}, & \text{otherwise.} \end{cases} \tag{2.7}$$

2.1 Uniform algebraic trigonometric tension B-spline

Here, we provide the UAT tension B-spline interpolation approach to obtaining a solution approximation to the problem defined by (2.4)-(2.5). To begin, we create uniform grids to partition the range $[0, 1]$. Assume $\Omega = \{0 = d_0, d_1, d_2, ..., d_n = 1\}$ be the regular split and $h_i = 1/n$, $(i = 1, 2, ..., n)$ denote the step size of the regular split of $[0, 1]$. To preserve the basis functions and interpolation points in the estimation of (2.4)-(2.5), we add two imaginary grid points along both ends of the split Ω. Then, the split Ω becomes $\Omega = \{d_{-2}, d_{-1}, d_0, ..., d_n, d_{n+1}\}$. By using the results in [36], we can conclude the explicit representation of the UAT tension B-spline basis function $\Phi_i(d)$ with tension parameter τ of order $l = 2$ as:

$$\Phi_{i,l}(d) = \begin{cases} \frac{\sin \tau(d-d_{i-2})}{\sin \tau h}, & d \in [d_{i-2}, d_{i-1}) \\ \frac{\sin \tau(d_i - d)}{\sin \tau h}, & d \in [d_{i-1}, d_i) \\ 0, & \text{otherwise.} \end{cases} \tag{2.8}$$

Now we suppose that $l \geq 3$, and present recurssive formula to get high order UAT tension B-spline basis function $\Phi_{i,l}(d)$ as:

$$\Phi_{i,l}(d) = \int_{-\infty}^{d} (H_{i,l-1} TB_{i,l-1}(s) - H_{i+1,l-1} TB_{i+1,l-1}(s))ds, \tag{2.9}$$

where $H_{i,l} = (\int_{-\infty}^{\infty} \Phi_{i,l-1}(s)ds)^{-1}$, $(i = 0, \pm 1, \pm 2, ...)$. If $\Phi_{i,l}(d) = 0$ then $H_{i,l}$, $\Phi_{i,l}(d)$ to satisfy

$$\int_{-\infty}^{d} H_{i,l} \Phi_{i,l}(z)dz = \begin{cases} 1, & d \geq d_{i+l} \\ 0, & d < d_{i+l}. \end{cases} \tag{2.10}$$

Using $\tau > 0$, if $\tau < \frac{\pi}{h}$ in equation (2.8), we get non-polynomial B-spline with tension parameter τ over the space $\{\cos \tau d, \sin \tau d, d^{k-3}, ..., d, 1\}$. Now, for $\tau > 0$ and $l = 5$ through using equations (2.8) and (2.9), we get a fourth order explicit representation of a non-polynomial B-spline with tension parameter τ as:

$$\Phi_{i,5}(d) = \rho \begin{cases} \frac{\tau^2 T_{i-2}^2 + 2C_{i-2} - 2}{2\tau^2}, & d \in [d_{i-2}, d_{i-1}) \\ \frac{-\tau^2(3h^2 + 6h\tau T_{i-2} + 2T_{i-2}^2 + 2M(\tau^2 T_{i-2}^2 - 2))(6C_{i-1} + 2C_i - 4)}{2\tau^2}, & d \in [d_{i-1}, d_i) \\ \frac{-\tau^2(13h^2 + 10h\tau T_{i-2} + 2T_{i-2}^2 + M(2\tau^2(11h^2 + 10hT_{i-2}^2)))}{2\tau^2} & \\ + \frac{4M\tau^2 T_{i-2}^2 - 8M + 6C_i + 6C_{i+1} - C_i}{2\tau^2}, & d \in [d_i, d_{i+1}) \\ \frac{-\tau^2(23h^2 + 14h\tau T_{i-2} + 2T_{i-2}^2 + 2M(\tau^2 T_{i-2}^2 - 2))(-2C_{i+1} + 6C_{i+2} - 4)}{2\tau^2}, & d \in [d_{i+1}, d_{i+2}) \\ \frac{\tau^2 T_{i+3}^2 + 2C_{i+3} - 2}{2\tau^2}, & d \in [d_{i+2}, d_{i+3}) \\ 0, & \text{otherwise.} \end{cases} \tag{2.11}$$

where $\rho = \frac{1}{2h^2(1-\cos(\tau h))}$, $C_{i+j} = \cos(\tau(d_{i+j} - d))$, $T_{i+j} = (d_{i+j} - d)$, and $M = \cos(\tau h)$. Let $\Phi_{i,5}(d)$ be the fourth order UAT tension B-splines interpolating function at the grid points d_i. Now, we define

$$Y(d) = \sum_{i=-2}^{n+1} \beta_i \Phi_{i,5}(d). \tag{2.12}$$

To be the numerical solution of considered problem (2.4)-(2.5), where β_i are unknown parameter and $\Phi_{i,5}(d)$ be fourth order UAT tension B-splines basis function. The values of the fourth order UAT tension B-splines, $\Phi_{i,5}(d)$ as well as their derivatives at the grid points, d_i is given in Table 1.

Table 1. The values of UAT tension B-splines basis function and $\Phi_{i,5}(d)$, $\Phi'_{i,5}(d)$ $\Phi''_{i,5}(d)$ $\Phi'''_{i,5}(d)$.

d	d_{i-2}	d_{i-1}	d_i	d_{i+1}	d_{i+2}	d_{i+3}
$\Phi_{i,5}(d)$	0	$\varkappa_1$	$\varkappa_2$	$\varkappa_2$	$\varkappa_1$	0
$\Phi'_{i,5}(d)$	0	$\varkappa_3$	$\varkappa_4$	$-\varkappa_4$	$-\varkappa_3$	0
$\Phi''_{i,5}(d)$	0	$\varkappa_5$	$\varkappa_6$	$\varkappa_6$	$\varkappa_5$	0
$\Phi'''_{i,5}(d)$	0	$\varkappa_7$	$\varkappa_8$	-$\varkappa_8$	$-\varkappa_7$	0

where,

$$\varkappa_1 = \rho\left(\frac{h^2\tau^2 + 2\cos(\tau h) - 2}{2\tau^2}\right),\ \varkappa_2 = \rho\left(\frac{(h^2\tau^2 - 2\cos(h\tau))(h^2\tau^2+1)+2}{2\tau^2}\right),$$
$$\varkappa_3 = \rho\left(\frac{h\tau - \sin(h\tau)}{\tau}\right),\ \varkappa_4 = \rho\left(\frac{-h\tau - 3\sin(h\tau) + 2h\tau\cos(h\tau)}{\tau}\right),$$
$$\varkappa_5 = \rho(1-\cos(h\tau)),\ \varkappa_6 = \rho(-1+\cos(h\tau)),$$
$$\varkappa_7 = \rho(\tau\sin(h\tau)),\ \varkappa_8 = -\rho(3\tau\sin(h\tau)).$$

Here each UAT tension B-spline function $\Phi_{i,5}(\omega_i),\ i = -2(-1)N$ includes five components on [0,1]. Therefore, from equation (2.11), we can express the values of Y_i, Y'_i, Y''_i and Y'''_i at grid points as a linear combination of unknown parameters and coefficients β_i such as:

$$Y(d_i) = \varkappa_1\beta_{i-2} + \varkappa_2\beta_{i-1} + \varkappa_2\beta_i + \varkappa_1\beta_{i+1} \tag{2.13}$$

$$Y'(d_i) = \varkappa_3\beta_{i-2} + \varkappa_4\beta_{i-1} - \varkappa_4\beta_i - \varkappa_3\beta_{i+1} \tag{2.14}$$

$$Y''(d_i) = \varkappa_5\beta_{i-2} - \varkappa_6\beta_{i-1} - \varkappa_6\beta_i + \varkappa_5\beta_{i+1} \tag{2.15}$$

$$Y'''(d_i) = \varkappa_7\beta_{i-2} + \varkappa_8\beta_{i-1} - \varkappa_8\beta_i - \varkappa_7\beta_{i+1} \tag{2.16}$$

since $Y(d)$ is a solution that is close to $W(d)$. Now, the difference equations (2.4) and (2.5) are given at the grid points by,

$$L(Y(d_i)) \equiv b(d_i)Y''(d_i) + e(d_i)Y'(d_i) = \frac{p(d_i)}{q(d_i)}g(d_i, Y(d_i), Y'(d_i)), \tag{2.17}$$

and

$$Y'(0) = 0, \qquad \omega_1 Y(1) + \omega_2 Y'(1) = \omega_3. \tag{2.18}$$

Now using the equations (2.12) in equation (2.17), we obtain:

$$b(d_i)\sum_{i=-2}^{n+1}\beta_i\Phi''_{i,5}(d_i) + e(d_i)\sum_{i=-2}^{n+1}\beta_i\Phi'_{i,5}(d_i) = \frac{p(d_i)}{q(d_i)}g\left(d_i, \sum_{i=-2}^{n+1}\beta_i\Phi_{i,5}(d_i), \sum_{i=-2}^{n+1}\beta_i\Phi'_{i,5}(d_i)\right), \tag{2.19}$$

with the boundary conditions

$$\sum_{i=-2}^{n+1}\beta_i\Phi'_{i,5}(0) = 0, \qquad \omega_1\sum_{i=-2}^{n+1}\beta_i\Phi_{i,5}(1) + \omega_2\sum_{i=-2}^{n+1}\beta_i\Phi'_{i,5}(1) = \omega_3. \tag{2.20}$$

The values of $\Phi_{i,5}(d_i)$ and their derivatives from equations (2.13)-(2.15) are substituted in equation (2.19), we obtain

$$d_i(\varkappa_5\beta_{i-2}-\varkappa_6\beta_{i-1}-\varkappa_6\beta_i+\varkappa_5\beta_{i+1})+e_i(\varkappa_3\beta_{i-2}+\varkappa_4\beta_{i-1}-\varkappa_4\beta_i-\varkappa_3\beta_{i+1})=\frac{p(d_i)}{q(d_i)}g\big(d_i,$$
$$(\varkappa_1\beta_{i-2}+\varkappa_2\beta_{i-1}+\varkappa_2\beta_i+\varkappa_1\beta_{i+1}),(\varkappa_3\beta_{i-2}+\varkappa_4\beta_{i-1}-\varkappa_4\beta_i-\varkappa_3\beta_{i+1})\big),\quad i=0,1,2,...,n. \tag{2.21}$$

$$(d_i\varkappa_5+e_i\varkappa_3)\beta_{i-2}+(-d_i\varkappa_6-e_i\varkappa_4)\beta_{i-1}+(-d_i\varkappa_6-e_i\varkappa_4)\beta_i+(d_i\varkappa_5+e_i\varkappa_3)\beta_{i+1}=\frac{p(d_i)}{q(d_i)}g\big(d_i,$$
$$(\varkappa_1\beta_{i-2}+\varkappa_2\beta_{i-1}+\varkappa_2\beta_i+\varkappa_1\beta_{i+1}),(\varkappa_3\beta_{i-2}+\varkappa_4\beta_{i-1}-\varkappa_4\beta_i-\varkappa_3\beta_{i+1})\big),\quad i=0,1,2,...,n. \tag{2.22}$$

and

$$\varkappa_3\beta_{-2}+\varkappa_4\beta_{-1}-\varkappa_4\beta_0-\varkappa_3\beta_1=0, \tag{2.23}$$
$$\omega_1(\varkappa_1\beta_{n-2}+\varkappa_2\beta_{n-1}+\varkappa_2\beta_n+\varkappa_1\beta_{n+1})+\omega_2(\varkappa_3\beta_{n-2}+\varkappa_4\beta_{n-1}-\varkappa_4\beta_n-\varkappa_3\beta_{n+1})=\omega_3. \tag{2.24}$$

We observed that the system of equations (2.22)-(2.25) cannot be solved uniquely. For the unique solution of the system of equations (2.22)-(2.25), we need one additional boundary equation. In order to accomplish this goal, we differentiate equation (2.17) with regard to the d, we get

$$b_iY'''(d)+\tilde{e}_iY''(d_i)+e_iY'(d_i)=\omega(d_i)g'(d_i,Y(d_i),Y'(d_i))(d_i,Y(d_i)Y'(d_i))$$
$$+\omega'(d_i)g(d_i,Y(d_i)Y'(d_i)), \tag{2.25}$$

where $\tilde{e}_i=d_i+e_i$ and $\omega_i=\frac{p(d_i)}{q(d_i)}$.
Using equations (2.13)-(2.16) in equation (2.25), at $i=0$, we obtain

$$b_i(\varkappa_7\beta_{i-2}+\varkappa_8\beta_{i-1}-\varkappa_8\beta_i-\varkappa_7\beta_{i+1})+\tilde{e}_i(\varkappa_5\beta_{i-2}-\varkappa_6\beta_{i-1}-\varkappa_6\beta_i+\varkappa_5\beta_{i+1})$$
$$e_i(\varkappa_3\beta_{i-2}+\varkappa_4\beta_{i-1}-\varkappa_4\beta_i-\varkappa_3\beta_{i+1})=\omega(d_i)g'(d_i,(\varkappa_1\beta_{i-2}+\varkappa_2\beta_{i-1}+\varkappa_2\beta_i+\varkappa_1\beta_{i+1}),$$
$$(\varkappa_3\beta_{i-2}+\varkappa_4\beta_{i-1}-\varkappa_4\beta_i-\varkappa_3\beta_{i+1}))(1,(\varkappa_3\beta_{i-2}+\varkappa_4\beta_{i-1}-\varkappa_4\beta_i-\varkappa_3\beta_{i+1}),$$
$$(\varkappa_5\beta_{i-2}+\varkappa_6\beta_{i-1}+\varkappa_6\beta_i+\varkappa_5\beta_{i+1}))+\omega'(d_i)((\varkappa_1\beta_{i-2}+\varkappa_2\beta_{i-1}+\varkappa_2\beta_i+\varkappa_1\beta_{i+1}),$$
$$(\varkappa_3\beta_{i-2}+\varkappa_4\beta_{i-1}-\varkappa_4\beta_i-\varkappa_3\beta_{i+1})). \tag{2.26}$$

From equations (2.22)-(2.26), we have found a system of $n+4$ equations and $n+4$ undetermined coefficients $\beta_{-2},\beta_{-1},\beta_0,...,\beta_{n-1},\beta_n,\beta_{n+1}$. On annihilating the undetermined coefficients $\beta_{-2},\beta_{-1},\beta_{n+1}$ from the equations (2.22)-(2.26), we get $n+1$ linear equations and $n+1$ undetermined coefficients, $\beta_0,\beta_1,...,\beta_{n-1},\beta_n$, which can be written in the matrix form as:

$$A\psi+F(\psi)=V, \tag{2.27}$$

where

$$A=\begin{pmatrix} D_1 & D_2 & 0 & 0 & 0 & 0 & 0 & 0 & 0 & 0 & \cdots & 0\\ D_3 & D_4 & \tilde{\psi}_2 & 0 & 0 & 0 & 0 & 0 & 0 & 0 & \cdots & 0\\ 0 & \tilde{\mu}_3 & \tilde{\omega}_3 & \tilde{\varsigma}_3 & \tilde{\psi}_3 & 0 & 0 & \cdots & \cdots & \cdots & \cdots & 0\\ 0 & 0 & \tilde{\mu}_4 & \tilde{\omega}_4 & \tilde{\varsigma}_4 & \tilde{\psi}_4 & 0 & 0 & \cdots & \cdots & \cdots & \cdots\\ \vdots & \vdots & \vdots & \vdots & \vdots & \vdots & \vdots & \vdots & \vdots & \vdots & \vdots & \vdots\\ 0 & 0 & 0 & \cdots & 0 & 0 & 0 & \tilde{\mu}_{n-1} & \tilde{\omega}_{n-1} & \tilde{\varsigma}_{n-1} & \tilde{\psi}_{n-1} & 0\\ 0 & 0 & 0 & 0 & \cdots & 0 & 0 & 0 & 0 & D_6 & D_7 & D_8 \end{pmatrix},$$

$$\psi = \begin{pmatrix} \beta_0 \\ \beta_1 \\ \beta_2 \\ \vdots \\ \vdots \\ \beta_{n-2} \\ \beta_{n-1} \\ \beta_n \end{pmatrix}, \qquad F(\psi) = \begin{pmatrix} F_0 \\ F_1 \\ F_2 \\ \vdots \\ \vdots \\ F_{n-2} \\ F_{n-1} \\ F_n \end{pmatrix}, \qquad V = \begin{pmatrix} \tilde{g}_0 \\ \tilde{g}_1 \\ \tilde{g}_2 \\ \vdots \\ \vdots \\ \tilde{g}_{n-2} \\ \tilde{g}_{n-1} \\ \tilde{g}_n \end{pmatrix},$$

and

$$\begin{aligned}
&D_1 = (\varrho_1 - \varrho_1 \varkappa_4), \quad D_2 = (\varrho_1 \varkappa_4 + \varrho_3), \quad D_3 = (\varrho_1 \varkappa_3 + \varrho_4), \\
&D_4 = \left(\varkappa_4 + \frac{D_2}{D_1}\right), \quad D_5 = \left(\varkappa_3 + \varkappa_4 \frac{D_3}{D_1}\right), \quad D_6 = \left(\tilde{\mu}_n - \frac{\tilde{\psi}_n \tilde{b}_1}{\tilde{b}_4}\right), \\
&D_7 = \left(\tilde{\omega}_n - \frac{\tilde{\psi}_n \tilde{b}_2}{\tilde{b}_4}\right), \quad D_8 = \left(\tilde{\varepsilon}_n - \frac{\tilde{\psi}_n \tilde{b}_1}{\tilde{b}_4}\right), \quad \tilde{g}_1 = \left(F_0 + \frac{\varkappa_4 F_0' \tilde{\mu}_1}{D_1} - \frac{\tilde{\omega}_1 F_0'}{D_1}\right), \\
&\tilde{g}_2 = \left(F_1 - \frac{\mu_2 \tilde{F}_0'}{D_1}\right), \quad \tilde{g}_3 = \left(F_n - \frac{\psi_2 \tilde{\omega}_n}{\tilde{b}_1}\right), \quad \tilde{\mu}_i = (d_i \varkappa_5 + e_i \varkappa_3), \\
&\tilde{\omega}_i = (-d_i \varkappa_6 - e_i \varkappa_4) \quad \tilde{\varsigma}_i = (-d_i \varkappa_6 - e_i \varkappa_4), \quad \tilde{\psi}_i = (d_i \varkappa_5 - e_i \varkappa_3).
\end{aligned}$$

With Newton's approach, we can find a solution to the preceding nonlinear system.

3 Numerical Examples(NE)

To validate our theoretical approach, we solved two nonlinear applications based on real-world situations. Moreover, the efficiency of the suggested approach was compared to that of existing techniques. To compute the maximum absolute errors, the following measures were used. (MAE) E_∞ and the L_2 norm error E_2 as:

$$E_2 = \sqrt{h \sum_{i=1}^{n} |Y(d_i) - W(d_i)|},$$

$$E_\infty = \max_{0 \le i \le n} |Y(d_i) - W(d_i)|.$$

The order of convergence (OC) can be obtained by applying the formula:

$$O_\infty = \frac{\log(E_\infty^n) - \log(E_\infty^{2n})}{\log(2)},$$

$$O_2 = \frac{\log(E_2^n) - \log(E_2^{2n})}{\log(2)}.$$

Example 3.1. Consider the generalized Thomas-Fermi type equation [13]

$$\begin{cases} -(d^\eta W'(d))' = \lambda d^{\eta+\lambda-2}(-dW'(d) - (\eta + \lambda - 1))e^{W(d)}, & d \in [0, 1] \\ W'(0) = 0, \quad W(1) = -\log(5). \end{cases} \tag{3.1}$$

The analytic solution of this NE is given by $Y(d) = \log\left(\frac{1}{4+d^\lambda}\right)$. We solved the equation (3.1) by applying the proposed interpolation approach applicable to a number of different types of n. The errors E_∞, E_2 as well as the computational rate of convergence of the proposed technique (2.27) are reported in the Tables 2 and 3. for $\eta = 0.25$ and $\eta = 0.75$, respectively. Based on the information in Tables 2 and 3, we may conclude that the OC of the suggested technique is two, which is the same as the conclusion from the theory. We have compared the E_∞, produced by the current approach (PM) to the results obtained by [13] in Table 4. These tables show that compared to the method in [13], where the number of grid points is kept constant, the PM yields less errors and a higher degree of convergence. Analytic and approximation solutions for $\eta = 0.25$ and $n = 64$ are presented in Fig.1 for visualisation and comparison. When comparing the proximity of two answers, we have provided both precise and approximate solutions at different magnification levels inside the graph. In addition, the absolute errors are shown for different values of $h = 0.0625, 0.03125, 0.0125, 0.00625$ in Fig.2. Errors are shown to diminish as n increases.

Table 2. Errors E_∞, E_2 and corresponding order of convergence of example 1, for $\eta = 0.5$ and $\lambda = 5$ with $\tau = 2$.

h	MAE(E_∞)			L_2 norm(E_2)		
	PM	Order	time(sec)	PM	Order	time(sec)
0.1	2.74×10^{-05}	$---$	0.276	1.52×10^{-05}	$---$	0.405
0.05	6.59×10^{-06}	2.2945	0.553	9.14×10^{-06}	2.3085	0.562
0.025	8.71×10^{-07}	2.6833	0.665	2.11×10^{-06}	2.1187	0.994
0.0125	1.78×10^{-07}	2.2891	0.962	4.46×10^{-07}	2.2424	1.023
0.00625	3.90×10^{-08}	2.1891	1.441	8.85×10^{-08}	2.3354	1.896

Table 3. Errors E_∞, E_2 and OC of NE 1, for $\eta = 0.25$ and $\lambda = 5$ with $\tau = 9$.

n	MAE(E_∞)			L_2 norm(E_2)		
	PM	Order	time(sec)	PM	Order	time(sec)
10	3.70×10^{-05}	$---$	0.235	1.52×10^{-05}	$---$	0.246
20	8.60×10^{-06}	2.1053	0.475	9.51×10^{-06}	2.5681	0.486
40	1.85×10^{-07}	2.2112	0.605	1.97×10^{-06}	2.2685	0.352
80	4.48×10^{-07}	2.0502	1.002	4.48×10^{-07}	2.1379	0.681
160	9.24×10^{-08}	2.2783	1.742	8.96×10^{-08}	2.3236	1.259

Table 4. Evaluation of the errors E_∞ of NE 1, for $\lambda = 5$.

h	$\eta = 0.25, \tau = 9$		$\eta = 0.5, \tau = 2$	
	PM	In[13]	PM	In[13]
10	3.70×10^{-05}	2.20×10^{-03}	2.74×10^{-05}	1.90×10^{-03}
20	8.60×10^{-06}	5.53×10^{-04}	6.59×10^{-06}	4.70×10^{-04}
40	1.85×10^{-07}	1.38×10^{-04}	8.71×10^{-07}	1.17×10^{-04}
80	4.48×10^{-07}	3.46×10^{-05}	1.78×10^{-07}	2.94×10^{-05}
160	9.24×10^{-08}	8.66×10^{-06}	3.90×10^{-08}	7.35×10^{-06}

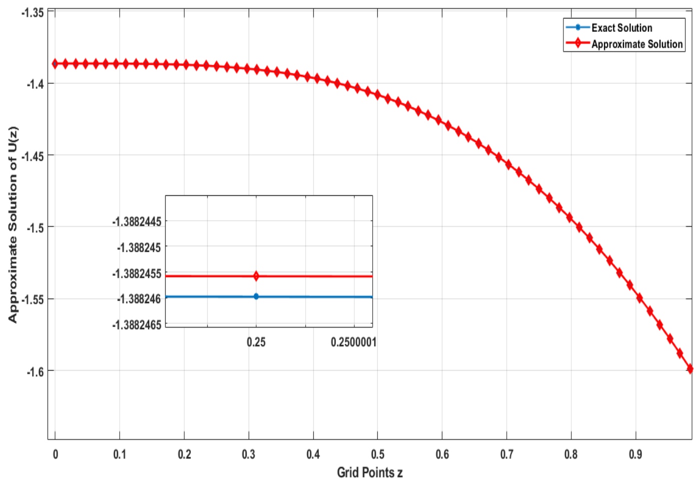

Figure 1. True and approximate outcomes of NE 1 for $n = 64$.

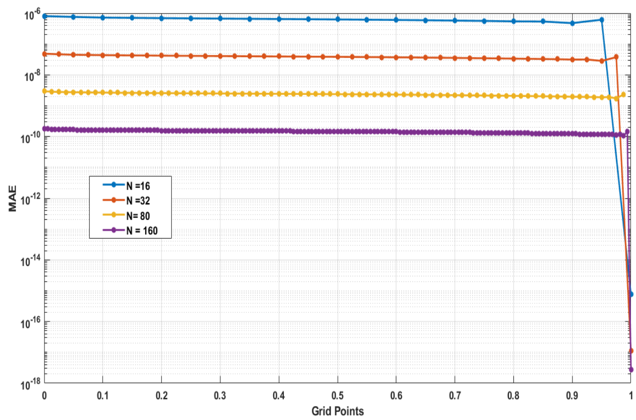

Figure 2. Logarithmic plot of error E_∞ of NE 1 for various values of $n = 16, 32, 80, 160$.

Example 3.2. Consider the generalized Thomas-Fermi type equation [13]

$$\begin{cases} -(\frac{d^\eta}{1+d^{\lambda-1}}W'(d))' = \frac{\lambda d^{\eta+\lambda-2}}{1+d^{\lambda-1}}(-dW'(d) - \frac{(\eta+\lambda-1)}{1+d^{\lambda-1}} - \frac{\eta d^{\lambda-1}}{1+d^{\lambda-1}})e^{W(d)}, & d \in [0,1] \\ W'(0) = 0, \quad W(1) = -\log(5) - \lambda. \end{cases} \tag{3.2}$$

The following expression provides an analytical solution to this NE $Y(d) = \log\left(\frac{1}{4+d^\lambda}\right)$. We use the suggested method (2.27) to solve the problem (3.2) when h is $0.0625, 0.03125, 0.015625, 0.0078125, 0.00390625$. For $\eta = 0.25$ and $\eta = 0.75$, the Tables 5 and 6 show the E_∞, E_2 errors and the OC of the proposed method (2.27). In order to prove that the current technique provides more accurate results than the approaches described in [13], we have performed comparison linking the errors E_∞ of our approach and those acquired by the UCS scheme in [13]. These findings can be found in Tables 7. We have displayed graphs for $\eta = 1/4$ and $n = 26$ in Fig.3, which demonstrate excellent conformity with the use of the true solution, so that we may see and implement the analytic and approximation solutions. You can see these graphs by clicking on Fig.3. Within the graph, we have also shown solutions for zoomed-in portions, both precise and approximate, to demonstrate the proximity between possible solutions. In addition, the absolute errors are shown in Fig.4, for a number of different values of $0.0625, 0.03125, 0.015625, 0.0078125$. It is shown that the errors become less severe as the value of n gets higher. Moreover, the absolute errors for different value of h is $0.0625, 0.03125, 0.015625, 0.0078125$ is shown in Fig.4. It can be seen that the errors becomes less whenever the value of h gets lower.

Table 5. Errors E_∞, E_2 and corresponding order of convergence of example 2, for $\eta = 0.25$ and $\lambda = 5$ with $\tau = 2$.

h	MAE(E_∞)			L_2 norm(E_2)		
	PM	Order	time(sec)	PM	Order	time(sec)
0.1	4.12×10^{-04}	$---$	0.229	6.12×10^{-05}	$---$	0.241
0.05	9.00×10^{-05}	2.1962	0.485	1.16×10^{-05}	2.3929	0.514
0.025	1.91×10^{-05}	2.2337	0.842	2.42×10^{-06}	2.2658	0.841
0.0125	3.56×10^{-06}	2.4255	1.462	5.19×10^{-07}	2.2228	1.965
0.00625	7.17×10^{-07}	2.3121	3.378	9.89×10^{-08}	2.3916	3.246

Table 6. Errors E_∞, E_2 and OC of NE 1, for $\eta = 0.5$ and $\lambda = 5$ with $\tau = 9$.

n	MAE(E_∞)			L_2 norm(E_2)		
	PM	Order	time(sec)	PM	Order	time(sec)
10	4.14×10^{-04}	$---$	0.256	2.17×10^{-04}	$---$	0.152
20	8.56×10^{-05}	2.2764	0.506	4.45×10^{-05}	2.2896	0.655
40	1.90×10^{-05}	2.1715	0.896	8.75×10^{-06}	2.3470	0.782
80	4.24×10^{-06}	2.1638	1.023	1.90×10^{-06}	2.0889	1.689
160	9.30×10^{-07}	2.1889	1.545	4.47×10^{-07}	2.3558	2.846

Table 7. Evaluation of the errors E_∞ of NE 1, for $\lambda = 5$.

h	$\eta = 0.25$, $\tau = 9$		$\eta = 0.5$, $\tau = 2$	
	PM	In[13]	PM	In[13]
10	3.26×10^{-05}	4.50×10^{-03}	2.32×10^{-05}	1.60×10^{-03}
20	1.99×10^{-06}	1.10×10^{-03}	1.40×10^{-06}	4.90×10^{-04}
40	1.23×10^{-07}	2.82×10^{-04}	8.72×10^{-07}	1.75×10^{-05}
80	7.69×10^{-08}	7.07×10^{-05}	5.43×10^{-08}	2.44×10^{-05}
160	4.80×10^{-09}	1.77×10^{-05}	3.39×10^{-09}	6.09×10^{-06}

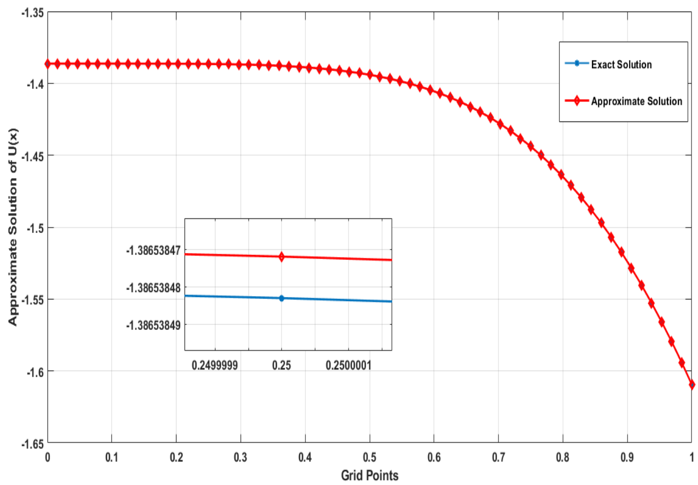

Figure 3. Analytic and approximate solution of example 2 for $N = 64$.

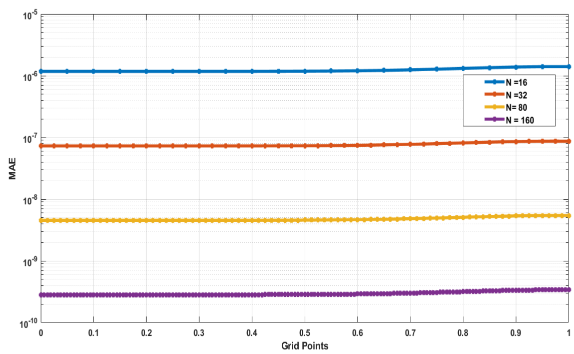

Figure 4. Logarithmic plot of error E_∞ of example 2 for various values $N = 16, 32, 80, 160$.

4 Conclusion

The objective of this study is the development of an appropriate and resilient numerical approach for solving modified Thomas-Fermi boundary value problems. Utilizing a uniform algebraic trigonometric tension B-spline basis function on a uniform mesh the method is developed. The fundamental benefit of the suggested technique is that it is efficient and robust, highly accurate, and simple to implement on the investigated issues. As the number of grid points rises, the positive outcomes may be enhanced. We used several real-world numerical experiments to demonstrate that the scheme that we devised is effective and worthy of consideration. From the graphs, it is clear that the numerical outcomes of this method matches the analytical outcomes well.

References

[1] L. H. Thomas, The calculation of atomic fields, in: Mathematical proceedings of the Cambridge philosophical society, vol. 23, Cambridge University Press1927, pp. 542–548.

[2] E. Fermi, Statistical method to determine some properties of atoms, in: Rendiconti Lincei 1927 (602-607).

[3] R. Pandey, A. K. Verma, On a constructive approach for derivative-dependent singular boundary value problems, in: International Journal of Differential Equations 2011 (2011).

[4] R. Pandey, A. K. Verma, On solvability of derivative dependent doubly singular boundary value problems, in: Journal of Applied Mathematics and Computing 33 (2010) (1-2) 489–511.

[5] Y. Zhang, Existence of solutions of a kind of singular boundary value problem, in: Nonlinear Analysis: Theory, Methods & Applications 21 (1993) (2) 153–159.

[6] Y. Zhang, A note on the solvability of singular boundary value problems, in: Nonlinear Analysis: Theory, Methods & Applications 26 (1996) (10) 1605–1609.

[7] D. Dunninger, J. C. Kurtz, Existence of solutions for some nonlinear singular boundary value problems, in: Journal of Mathematical Analysis and Applications 115 (1986) (2) 396–405.

[8] S. Iyengar, P. Jain, Spline finite difference methods for singular two point boundary value problems, in: Numerische Mathematik 50 (1986) 363–376.

[9] M. Chawla, C. Katti, Finite difference methods and their convergence for a class of singular two point boundary value problems, in: Numerische Mathematik 39 (1982) 341–350.

[10] M. Kumar, A three-point finite difference method for a class of singular two-point boundary value problems, in: Journal of computational and applied mathematics 145 (2002) (1) 89–97.

[11] A. R. Kanth, Cubic spline polynomial for non-linear singular two-point boundary value problems, in: Applied mathematics and computation 189 (2007) (2) 2017–2022.

[12] J. Rashidinia, Z. Mahmoodi, M. Ghasemi, Parametric spline method for a class of singular two-point boundary value problems, in: Applied mathematics and computation 188 (2007) (1) 58–63.

[13] P. Roul, V. P. Goura, B-spline collocation methods and their convergence for a class of nonlinear derivative dependent singular boundary value problems, in: Applied Mathematics and Computation 341 (2019) 428–450.

[14] M. P. Alam, D. Kumar, A. Khan, Trigonometric quintic B-spline collocation method for singularly perturbed turning point boundary value problems, in: International Journal of Computer Mathematics 98 (2021) (5) 1029–1048.

[15] M. P. Alam, A. Khan, D. Baleanu, A high-order unconditionally stable numerical method for a class of multi-term time-fractional diffusion equation arising in the solute transport models, in: International Journal of Computer Mathematics 100 (2023) (1) 105–132.

[16] M. P. Alam, T. Begum, A. Khan, A new spline algorithm for solving non-isothermal reaction diffusion model equations in a spherical catalyst and spherical biocatalyst, in: Chemical Physics Letters 754 (2020) 137651.

[17] M. P. Alam, T. Begum, A. Khan, A high-order numerical algorithm for solving Lane–Emden equations with various types of boundary conditions, in: Computational and Applied Mathematics 40 (2021) 1–28.

[18] M. P. Alam, A. Khan, A high-order numerical method for solving nonlinear derivative-dependent singular boundary value problems using trigonometric B-spline basis function, in: Mathematical Sciences (2023) 1–17.

[19] S. Khuri, A. Sayfy, Numerical solution for the nonlinear Emden–Fowler type equations by a fourth-order adaptive method, in: International Journal of Computational Methods 11 (2014) (01) 1350052.

[20] P. Roul, K. Thula, A fourth-order B-spline collocation method and its error analysis for Bratu-type and Lane–Emden problems, in: International Journal of Computer Mathematics 96 (2019) (1) 85–104.

[21] A. K. Verma, S. Kayenat, On the convergence of Mickens' type nonstandard finite difference schemes on Lane-Emden type equations, in: Journal of Mathematical Chemistry 56 (2018) 1667–1706.

[22] M. Singh, A. K. Verma, R. P. Agarwal, On an iterative method for a class of 2 point & 3 point nonlinear sbvps, in: J. Appl. Anal. Comput 9 (2019) (4) 1242–1260.

[23] R. Singh, N. Das, J. Kumar, The optimal modified variational iteration method for the Lane-Emden equations with Neumann and Robin boundary conditions, in: The European Physical Journal Plus 132 (2017) 1–11.

[24] K. Parand, M. Dehghan, A. Rezaei, S. Ghaderi, An approximation algorithm for the solution of the nonlinear Lane–Emden type equations arising in astrophysics using Hermite functions collocation method, in: Computer Physics Communications 181 (2010) (6) 1096–1108.

[25] R. Singh, J. Kumar, G. Nelakanti, New approach for solving a class of doubly singular two-point boundary value problems using Adomian decomposition method, in: Advances in numerical analysis 2012 (2012).

[26] K. Parand, M. Dehghan, A. Pirkhedri, The Sinc-collocation method for solving the Thomas–Fermi equation, in: Journal of Computational and Applied Mathematics 237 (2013) (1) 244–252.

[27] R. Pandey, A. K. Singh, On the convergence of a fourth-order method for a class of singular boundary value problems, in: Journal of computational and applied mathematics 224 (2009) (2) 734–742.

[28] R. Pandey, A. K. Singh, On the convergence of a finite difference method for a class of singular boundary value problems arising in physiology, in: Journal of Computational and Applied Mathematics 166 (2004) (2) 553–564.

[29] P. Roul, V. P. Goura, R. Agarwal, A compact finite difference method for a general class of nonlinear singular boundary value problems with Neumann and Robin boundary conditions, in: Applied Mathematics and Computation 350 (2019) 283–304.

[30] J. Shahni, R. Singh, Laguerre wavelet method for solving Thomas–Fermi type equations, in: Engineering with Computers 38 (2022) (4) 2925–2935.

[31] R. Singh, J. Kumar, G. Nelakanti, Numerical solution of singular boundary value problems using Green's function and improved decomposition method, in: Journal of Applied Mathematics and Computing 43 (2013) 409–425.

[32] M. Turkyilmazoglu, Solution of initial and boundary value problems by an effective accurate method, in: International Journal of Computational Methods 14 (2017) (06) 1750069.

[33] A. K. Verma, D. Tiwari, Higher resolution methods based on quasilinearization and Haar wavelets on Lane–Emden equations, in: International Journal of Wavelets, Multiresolution and Information Processing 17 (2019) (03) 1950005.

[34] M. A. Z. Raja, J. Mehmood, Z. Sabir, A. K. Nasab, M. A. Manzar, Numerical solution of doubly singular nonlinear systems using neural networks-based integrated intelligent computing, in: Neural Computing and Applications 31 (2019) 793–812.

[35] R. Singh, J. Kumar, The Adomian decomposition method with Green's function for solving nonlinear singular boundary value problems, in: Journal of Applied Mathematics and Computing 44 (2014) 397–416.

[36] G. Wang, et al., Unified and extended form of three types of splines, in: Journal of computational and applied mathematics 216 (2008) (2) 498–508.

[37] J. Shahni, R. Singh, Numerical results of Emden–Fowler boundary value problems with derivative dependence using the Bernstein collocation method, in: Engineering with Computers 38 (2022) (Suppl 1) 371–380.

[38] R. Singh, J. Kumar, G. Nelakanti, Approximate series solution of singular boundary value problems with derivative dependence using Green's function technique, in: Computational and Applied Mathematics 33 (2014) 451–467.

Author information

Geetan Manchanda, Department of Mathematics, Maitreyi College, New Delhi-110021, India.
E-mail: gkhurana@maitreyi.du.ac.in

Zainav Khatoon, Department of Mathematics, Jamia Millia Islamia, New Delhi-110025, India.
E-mail: zainavk@gmail.com

Mohammad Prawesh Alam*, Department of Mathematics, Maitreyi College, New Delhi-110021, India.
E-mail: praweshalam15@gmail.com